EPJ Web of Conferences **109**, 02001 (2016)
DOI: 10.1051/epjconf/201610902001

Astrophysical site(s) of *r*-process elements in galactic chemo-dynamical evolution model

Yutaka Hirai[1,2,a,b], Yuhri Ishimaru[3], Takayuki R. Saitoh[4], Michiko S. Fujii[1,2], Jun Hidaka[5,2], and Toshitaka Kajino[2,1]

[1] *Department of Astronomy, Graduate School of Science, The University of Tokyo, 7-3-1 Hongo, Bunkyo-ku, Tokyo 113-0033, Japan*
[2] *Division of Theoretical Astronomy, National Astronomical Observatory of Japan, 2-21-1 Osawa, Mitaka, Tokyo 181-8588, Japan*
[3] *Department of Material Science, International Christian University, 3-10-2 Osawa, Mitaka, Tokyo 181-8585, Japan*
[4] *Earth-Life Science Institute, Tokyo Institute of Technology, 2-12-1 Ookayama, Meguro-ku, Tokyo 152-8551, Japan*
[5] *School of Science and Engineering, Meisei University, 2-1-1 Hodokubo, Hino, Tokyo 191-0042, Japan*

Abstract. Astrophysical site(s) of rapid neutron-capture process (*r*-process) is (are) not identified yet. Although core-collapse supernovae have been regarded as one of the possible candidates of the astrophysical site of *r*-process, nucleosynthesis studies suggest that serious difficulties in core-collapse supernovae to produce heavy elements with mass number of $\gtrsim$110. Recent studies show that neutron star mergers (NSMs) can synthesize these elements due to their neutron rich environment. Some chemical evolution studies of the Milky Way halo, however, hardly reproduce the observed star-to-star scatters of the abundance ratios of *r*-process elements (e.g., Eu) in extremely metal-poor stars. This is because of their low rate ($\sim 10^{-4}$ yr^{-1} for a Milky Way size galaxy) and long merger time ($\gtrsim$ 100 Myr). This problem might be solved if the stars in the Galactic halo are consisted of the stars formed in dwarf galaxies where the star formation efficiencies were very low. In this study, we carry out numerical simulations of galactic chemo-dynamical evolution using an *N*-body/smoothed particle hydrodynamics code. We construct detailed chemo-dynamical evolution model for the Local Group dwarf spheroidal galaxies (dSphs) assuming that the NSMs are the major source of *r*-process elements. Our models successfully reproduce the observed dispersion in [Eu/Fe] as a function of [Fe/H] if we set merger time of NSMs, $\lesssim$ 300 Myr with the Galactic NSM rate of $\sim 10^{-4}$ yr^{-1}. In addition, our results are consistent with the observed metallicity distribution of dSphs. In the early phase ($\lesssim$1 Gyr) of galaxy evolution is constant due to low star formation efficiency of dSphs. This study supports the idea that NSMs are the major site of *r*-process nucleosynthesis.

[a] Research Fellow of Japan Society for the Promotion of Science
[b] e-mail: yutaka.hirai@nao.ac.jp

1 Introduction

Astrophysical site(s) of rapid neutron-capture process (*r*-process) is (are) one of the open questions throughout half a century. Astronomical high dispersion spectroscopy observations show that extremely metal-poor stars with [Fe/H] $\lesssim -3$ have large star-to-star scatters in the ratio of *r*-process elements to iron [e.g. 1–3]. This observational feature gives us clues to understanding astrophysical site(s) of *r*-process.

Core-collapse supernovae (CCSNe) and neutron star mergers (NSMs) are candidates of astrophysical site(s) of *r*-process. CCSNe have long been suggested as a promising site of *r*-process [e.g., 4–7]. Recent studies however suggest that it is difficult to find conditions to synthesize *r*-process elements with mass number heavier than 110 [e.g., 8–11].

On the other hand, detailed nucleosynthesis calculations suggest that NSMs can synthesize these heavy *r*-process elements [e.g., 12–14]. Previous galactic chemical evolution studies however pointed out that NSMs hardly reproduce the observed large star-to-star scatters of extremely metal-poor stars by NSMs due to their long merger time ($\gtrsim$ 100 Myr) and low occurrence rate ($\sim 10^{-4}$ yr^{-1} for a Milky Way size galaxy) [15–17]. Several recent chemical evolution studies also require unlikely short merger time of NSMs ($\lesssim$ 10 Myr) or SNe to reproduce the observation [18–20].

This problem may be solved by calculating the chemical evolution according to the hierarchical merging paradigm. Ishimaru et al. (2015) suggest that NSMs with long merger time ($\sim$ 100 Myr) can account for the observation if the Milky Way halo was formed from sub-haloes with lower star formation efficiency in smaller mass sub-haloes [21]. Hydrodynamical simulations of galaxy formation also suggest that it is possible to reproduce the observation by NSMs with merger time of 100 Myr [22, 23]. However, high resolution models of van de Voort et al. (2015) suggest that it is difficult to reproduce the observation by NSMs with long merger time. In addition, it has not been clear how the merger time affects the final abundance pattern of *r*-process elements.

In this study, we aim to clarify the enrichment history of *r*-process elements by NSMs of different merger time using high-resolution *N*-body/smoothed particle hydrodynamics (SPH) simulations. We perform a series of simulations of dwarf spheroidal galaxies (dSphs) which would be building blocks of the Milky Way. The mass of one gas particle ($m_{\rm gas}$) is $4.0 \times 10^2 M_\odot$, which is 1 dex higher mass resolution than the highest resolution model of van de Voort et al. (2015) [22] ($m_{\rm gas} = 7.1 \times 10^3 M_\odot$). In this paper, we discuss the effects of the merger time of NSMs with high resolution simulations.

2 Method and models

2.1 *N*-body/smoothed particle hydrodynamics code, ASURA

We perform a series of simulations using an *N*-body/SPH code, ASURA [24, 25]. Details of the implementation of the code are described in Hirai et al. (2015) [26]. Gravity and hydrodynamics are computed using tree method [27] and SPH [28–30], respectively. Metallicity dependent cooling/heating function generated by Cloudy [31, 32] from 10 K to 10^9 K is adopted in this study. We adopt three kinds of particles in our simulation (dark matter, gas, and star). Dark matter particles are treated as collisionless particles to compute gravity. Gas particles are treated as SPH particles for hydrodynamics calculation. To compute chemical evolution and supernova feedback, we treat star particles as single stellar population (SSP) particles, i.e., each star particle is assumed to be an assembly of stars with the same age and metallicity.

For star formation, we require three conditions for gas particles: converging flow, high density (> 100 cm^{-3}), and low temperature (< 1000 K) following Saitoh et al. (2008) [24]. When a gas particle satisfies these conditions, one third of the mass of a gas particle is converted into a newly formed star particle. For metallicity of newly formed stars, we adopt an average metallicity of surrounding gas particles in a star forming region [26]. This is interpreted as a simple metal mixing. Hirai et al. (2015) [26] discuss the effect of metal mixing to the enrichment of *r*-process elements. We adopt the Salpeter initial mass function inside a star particle [33]. We assume that stars with a mass of 8–40 $M_\odot$ explode as CCSNe and distribute thermal energy of 10^{51} erg and chemical elements to surrounding gas particles. We adopt nucleosynthesis yields of Nomoto et al. (2006) [34]. We implement NSMs in the same way as CCSNe. We assume that 1 % of stars with a mass of 8–20 $M_\odot$ cause NSMs with the yield of $10^{-2} M_\odot$ for all *r*-process elements. This corresponds to the rate of 10^{-4} yr^{-1} for a Milky Way size galaxy which is consistent with the observational estimates [35]. We set merger time of NSMs (t_{NSM}) from 10 Myr to 500 Myr. Since 97 % of the number of Europium (Eu) is produced by *r*-process [36], we regard it as a representative of *r*-process elements. Table 1 lists the name of models and adopted merger time.

Table 1. Lists of models.

Model	t_{NSM} (Myr)
m010	10
m100	100
m500	500

2.2 Isolated dwarf spheroidal galaxy models

In this study, we assume isolated dSph models following Revaz et al. (2009); Revaz & Jablonka (2012) [37, 38]. Both dark matter and gas particles are distributed following the pseudo-isothermal profile,

$$\rho = \frac{\rho_{\mathrm{c}}}{1 + (r/r_{\mathrm{c}})^2}, \tag{1}$$

where ρ is the density of the galaxy model, ρ_{c} is the central density, and r_{c} is the core radius. The total mass of the galaxy (M_{tot}) is determined by the following equation,

$$M_{\mathrm{tot}} = 4\pi\rho_{\mathrm{c}} r_{\mathrm{c}}^3 \left[\frac{r_{\mathrm{max}}}{r_{\mathrm{c}}} - \arctan\left(\frac{r_{\mathrm{max}}}{r_{\mathrm{c}}}\right)\right], \tag{2}$$

where r_{max} is maximum outer radius. We set $M_{\mathrm{tot}} = 7.0 \times 10^8 M_\odot$, $r_{\mathrm{c}} = 1.0$ kpc, and $r_{\mathrm{max}} = 7.1$ kpc. The initial total number of particles in all models is 524,288. The mass of one dark matter and gas particle are $2.3 \times 10^3 M_\odot$ and $4.0 \times 10^2 M_\odot$, respectively. We set the gravitational softening length as 7 pc for all models.

3 Results

Figure 1 shows the metallicity ([Fe/H][1]) distribution of our model. As shown in this figure, the calculated metallicity distribution reproduces the observation. Since we only vary the merger time of NSMs, which does not affect the Fe abundance, metallicity distributions are the same for all models. In addition to the metallicity distribution, we have checked that velocity dispersion and time variation

[1] $[\mathrm{A/B}] = \log_{10}(N_{\mathrm{A}}/N_{\mathrm{B}}) - \log_{10}(N_{\mathrm{A}}/N_{\mathrm{B}})_\odot$, where N_{A} and N_{B} are number densities of elements A and B, respectively.

of the star formation rate are consistent with the observed dSphs. Star formation rate for the first 1 Gyr from the beginning of the simulation is $\lesssim 10^{-3} M_{\odot}\mathrm{yr}^{-1}$. Due to this low star formation rate, chemical evolution of dSphs is expected to be slow. Detailed chemo-dynamical properties of dSph models are discussed in Hirai et al. (2015) [26].

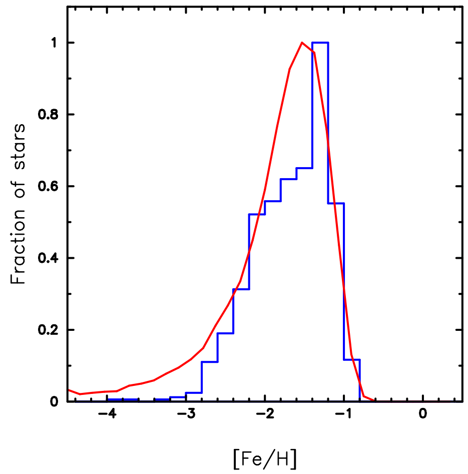

Figure 1. Metallicity distribution. Red curve represents metallicity distribution produced by our model. Blue histogram represents observed metallicity distribution of the Sculptor dSphs [39].

Figure 2 shows [Eu/Fe] as a function of [Fe/H]. As shown in this figure, most of the stars with Eu appears at [Fe/H] ~ -3 in models with $t_{\mathrm{NSM}} \leq 100$ Myr while most of the stars with Eu appears at [Fe/H] ~ -2.5 in model m500 ($t_{\mathrm{NSM}} = 500$ Myr). This figure shows even models with $t_{\mathrm{NSM}} \sim 100$ Myr is consistent with the observation. Existence of NSMs with $t_{\mathrm{NSM}} \sim 100$ Myr is supported by the observed binary pulsars [35] as well as population synthesis calculations [e.g., 42]. In contrast, existence of NSMs with $t_{\mathrm{NSM}} \sim 10$ Myr highly depends on the treatment of common envelope phase which is not well understood in population synthesis calculations [e.g., 42].

4 Discussion

In the last section, we have shown that models with $t_{\mathrm{NSM}} \leq 100$ Myr are consistent with observation. This result suggests that NSMs with merger time of ~ 100 Myr can be the astrophysical site of *r*-process. On the other hand, several chemical evolution studies suggest that it is difficult to reproduce the observation using NSMs with $t_{\mathrm{NSM}} \sim 100$ Myr [e.g., 15–20]. This is related to the difference in star formation efficiency among these models. Since we consider dSphs, the star formation efficiency of the early phase ($\lesssim 1$ Gyr) is < 0.1 Gyr^{-1} [26]. On the other hand, star formation efficiencies typically adopted in previous studies are 0.1– 1 Gyr^{-1}, resulting in the lack of metal-poor stars polluted by Eu. Due to the low star formation efficiency in this model, chemical evolution in the early phase is expected to be slow.

Figure 3 shows [Fe/H] as a function of time from the beginning of the major star formation. According to this figure, metallicity is constant ([Fe/H]~ -3) over 300 Myr. In this epoch, metallicity is determined by the yield of each SN rather than the number of SNe. This result suggests that Eu appears at [Fe/H] ~ -3 if the merger time of NSMs less than 300 Myr.

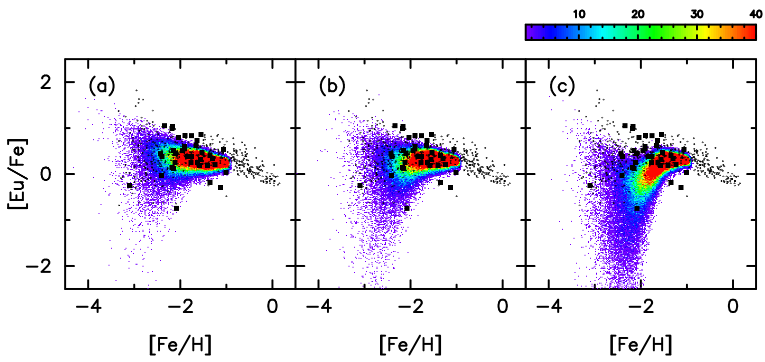

Figure 2. [Eu/Fe] as a function of [Fe/H]. (a) Model m010 ($t_{\rm NSM}$ = 10 Myr). (b) Model m100 ($t_{\rm NSM}$ = 100 Myr). (c) Model m500 ($t_{\rm NSM}$ = 500 Myr). Contours represent the number of stars produced by our models between 1 (purple) to 40 (red). Squares and small circles represent observed abundance of stars in dSphs and the Milky Way [SAGA database, 40, 41]. We exclude stars in the Fornax dSph due to extremely strong contribution of *s*-process. We also exclude carbon enhanced stars which may be affected by binary mass transfer.

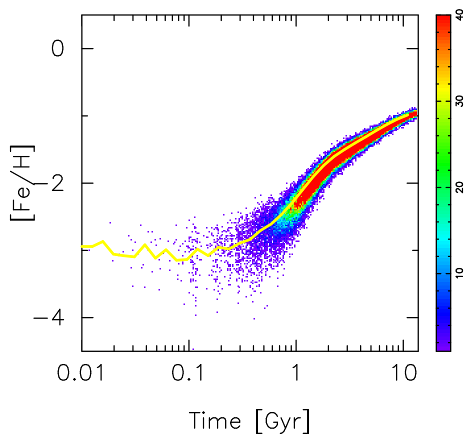

Figure 3. Age-metallicity relation. Contours represent the number of stars produced by our model. Yellow curve represents the average of metallicity in our models.

5 Summary

In this study, we have investigated the enrichment of *r*-process elements in isolated dSph models with a fixed mass by a series of *N*-body/SPH simulations. The results suggest that NSMs with merger time of $\lesssim$ 300 Myr can be the site of *r*-process. However, the effects of mass and density of dSphs to the enrichment of *r*-process elements are not understood yet. We will discuss how the mass and density of galaxies affect the enrichment history of *r*-process elements in the forthcoming paper.

This work is supported in part by MEXT SPIRE and JICFuS. Y. H. is financially supported by Grant-in-Aid for JSPS Fellows (15J00548). The authors are financially supported by JSPS Grants-in-Aid for Scientific Research (YI: 26400232, TRS: 26707007, MSF: 26800108, TK: 26105517, 24340060, 15H03665). Numerical computations and analysis were in part carried out on Cray XC30 and computers at CfCA, NAOJ.

References

[1] Honda, S., Aoki, W., Kajino, T., et al., ApJ **607**, 474 (2004)

[2] François, P., Depagne, E., Hill, V. et al., A&A **476**, 935 (2007)

[3] Sneden, C., Cowan, J. J., & Gallino, R., ARA&A **46**, 241 (2008)

[4] Meyer, B. S., Mathews, G. J., Howard, W. M., Woosley, S. E., & Hoffman, R. D., ApJ **399**, 656 (1992)

[5] Qian, Y.-Z., & Woosley, S. E., ApJ **471**, 331 (1996)

[6] Wanajo, S., Kajino, T., Mathews, G. J., & Otsuki, K., ApJ **554**, 578 (2001)

[7] Ishimaru, Y., Wanajo, S., Aoki, W., & Ryan, S. G., ApJL **600**, L47 (2004)

[8] Wanajo, S., Janka, H-T., & Müller, B., ApJL **726**, L15 (2011)

[9] Martínez-Pinedo, G., Fischer, T., Lohs, A., & Huther, L., PhRvL **109**, 251104 (2012)

[10] Fischer, T., Martínez-Pinedo, G., Hempel, M., & Liebendörfer, M., PhRvD **85**, 083003 (2012)

[11] Wanajo, S., ApJL **770**, L22 (2013)

[12] Bauswein, A., Goriely, S., & Janka, H.-T., ApJ **773**, 78 (2013)

[13] Rosswog, S., Korobkin, O., Arcones, A., Thielemann, F.-K., & Piran, T., MNRAS **439**, 744 (2014)

[14] Wanajo, S., Sekiguchi, Y., Nishimura, N., et al., ApJL **789**, L39 (2014)

[15] Mathews, G. J., & Cowan, J. J., Nature **345**, 491 (1990)

[16] Qian, Y.-Z., ApJL **534**, L67 (2000)

[17] Argast, D., Samland, M., Thielemann, F.-K., & Qian, Y.-Z., A&A **416**, 997 (2004)

[18] Matteucci, F., Romano, D., Arcones, A., Korobkin, O., & Rosswog, S., MNRAS **438**, 2177 (2014)

[19] Cescutti, G., Romano, D., Matteucci, F., Chiappini, C., & Hirschi, R., A&A **577**, A139 (2015)

[20] Wehmeyer, B., Pignatari, M., & Thielemann, F.-K., MNRAS **452**, 1970 (2015)

[21] Ishimaru, Y., Wanajo, S., & Prantzos, N., ApJL **804**, L35 (2015)

[22] van de Voort, F., Quataert, E., Hopkins, P. F., Kereš, D., & Faucher-Giguère, C.-A., MNRAS **447**, 140 (2015)

[23] Shen, S., Cooke, R., Ramirez-Ruiz, E., Madau, P., Mayer, L., & Guedes, J., ApJ **807**, 115 (2015)

[24] Saitoh, T. R., Daisaka, H., Kokubo, E., et al., PASJ **60**, 667 (2008)

[25] Saitoh, T. R., Daisaka, H., Kokubo, E., et al., PASJ **61**, 481 (2009)

[26] Hirai, Y., Ishimaru, Y., Saitoh, T. R., Fujii, M. S., Hidaka, J., & Kajino, T., ApJ **814**, 41 (2015)

[27] Barnes, J. & Hut, P., Nature **324**, 446 (1986)

[28] Lucy, L. B., AJ **82**, 1013 (1977)

[29] Gingold, R. A., & Monaghan, J. J., MNRAS **181**, 375 (1977)

[30] Monaghan, J. J., & Lattanzio, J. C., A&A **149**, 135 (1985)

[31] Ferland, G. J., Korista, K. T., Verner, D. A., et al., PASP **110**, 761 (1998)

[32] Ferland, G. J., Porter, R. L., van Hoof, P. A. M, et al., RMxAA **49**, 137 (2013)

[33] Salpeter, E. E., ApJ **121**, 161 (1955)

[34] Nomoto, K., Tominaga, N., Umeda, H., Kobayashi, C., & Maeda, K., Nucl. Phys. A **777**, 424 (2006)

[35] Lorimer, D. R., LRR **11**, 8 (2008)

[36] Burris, D. L., Pilachowski, C. A., Armandroff, T. E., et al., ApJ **544**, 302 (2000)
[37] Revaz, Y., Jablonka, P., Sawala, T., et al., A&A **501**, 189 (2009)
[38] Revaz, Y., & Jablonka, P., A&A **538**, A82 (2012)
[39] Kirby, E. N., Guhathakurta, P., Simon, J. D., et al., ApJS **191**, 352 (2010)
[40] Suda, T., Katsuta, Y., Yamada, S., et al., PASJ **60**, 1159 (2008)
[41] Suda, T., Hidaka, J., Ishigaki, M., et al., Mem. Soc. Astron. Italiana **85**, 600 (2014)
[42] Dominik, M., Belczynski, K., Fryer, C., et al, ApJ **759**, 52 (2012)